European Journal of Human Genetics (2009) 17, 301 – 310

www.nature.com/ejhg

ARTICLE

A reliable cell-based assay for testing unclassified *TSC2* gene variants

Ricardo Coevoets[1], Sermin Arican[1], Marianne Hoogeveen-Westerveld[1], Erik Simons[1], Ans van den Ouweland[1], Dicky Halley[1] and Mark Nellist*[,1]

[1]*Department of Clinical Genetics, Erasmus Medical Centre, Rotterdam, The Netherlands*

Tuberous sclerosis complex (TSC) is characterised by seizures, mental retardation and the development of hamartomas in a variety of organs and tissues. The disease is caused by mutations in either the *TSC1* gene or the *TSC2* gene. The *TSC1* and *TSC2* gene products, TSC1 and TSC2, form a protein complex that inhibits signal transduction to the downstream effectors of the mammalian target of rapamycin (mTOR). We have developed a straightforward, semiautomated in-cell western (ICW) assay to investigate the effects of amino acid changes on the TSC1–TSC2-dependent inhibition of mTOR activity. Using this assay, we have characterised 20 TSC2 variants identified in individuals with TSC or suspected of having the disease. In 12 cases, we concluded that the identified variant was pathogenic. The ICW is a rapid, reproducible assay, which can be applied to the characterisation of the effects of novel TSC2 variants on the activity of the TSC1–TSC2 complex.
European Journal of Human Genetics (2009) **17,** 301–310; doi:10.1038/ejhg.2008.184; published online 15 October 2008

Keywords: tuberous sclerosis complex; in-cell western; unclassified variants

Introduction

Tuberous sclerosis complex (TSC) is an autosomal dominant disorder characterised by seizures, mental retardation and the development of hamartomas in a variety of organs and tissues.[1] The disease is caused by mutations in either the *TSC1* gene on chromosome 9q34[2] or the *TSC2* gene on chromosome 16p13.3.[3] The *TSC1* and *TSC2* gene products, TSC1 and TSC2, form a protein complex that acts as a GTPase-activating protein (GAP) for the rheb GTPase, preventing the rheb-GTP-dependent stimulation of the mammalian target of rapamycin (mTOR).[4] In cells lacking either *TSC1* or *TSC2*, the downstream targets of mTOR, including p70 S6 kinase (S6K) and ribosomal protein S6, are constitutively phosphorylated.[5,6] The identification of the role of the TSC1–TSC2 complex in regulating mTOR has made it possible to compare the activity of different TSC1 and TSC2 variants. The effects of amino acid changes on TSC1–TSC2 complex formation, on the activation of rheb GTPase activity, and on the phosphorylation status of the downstream effectors of mTOR, can be determined.[7]

Comprehensive screens for mutations at the *TSC1* and *TSC2* loci have been performed in large cohorts of TSC patients.[8–11] In most studies ~20% of the identified mutations are either missense changes or small, in-frame insertions/deletions, predominantly in the *TSC2* gene. In some cases, when a missense change cosegregates with TSC, or when key relatives are not available for testing, it is difficult to establish whether the identified nucleotide change is a pathogenic mutation or a neutral variant. We identified a number of variants where it was not clear from the genetic data whether the identified variant was pathogenic or not.[10] To resolve some of these cases we tested the activity of the variant TSC1–TSC2 complexes using a variety of biochemical assays.[12]

To simplify and standardise the testing of TSC2 variants we have developed and tested an in-cell western (ICW) assay to determine whether specific *TSC2* sequence variants identified in individuals with, or suspected of having, TSC are disease

*Correspondence: Dr M Nellist, Department of Clinical Genetics, Erasmus Medical Centre, Dr Molewaterplein 50, 3015 GE Rotterdam, The Netherlands.
Tel: +31 10 7043357; Fax: +31 10 7049489;
E-mail: m.nellist@erasmusmc.nl
Received 15 April 2008; revised 9 July 2008; accepted 4 September 2008; published online 15 October 2008

causing. The ICW assay utilises secondary antibodies conjugated with near infrared fluorophores in combination with an infrared scanner enabling two distinct antibody signals to be detected simultaneously and quantified in fixed cells. The advantage of the ICW assay over immunoblot-based techniques is that no blotting step is required and the analysis and quantification can be performed directly in high-throughput multiwell plate formats. Therefore, the ICW assay streamlines both the experimental procedure and data analysis.

In-cell western assays to assess protein phosphorylation have been described previously.[13] However, in most reports, the effects of different pharmacological reagents have been monitored.[14] Here, we describe a transfection-based ICW assay to facilitate the characterisation of the effects of genetic changes in the *TSC2* gene on the activity of the TSC1–TSC2 complex and the mTOR signalling pathway. We have used this assay to characterise 20 TSC2 variants. Twelve variants (60%) did not inhibit mTOR activity in either the ICW assay or in a conventional immunoblot assay, and could therefore be classified as pathogenic mutations. Furthermore, we show that the ICW assay of TSC1–TSC2 function is amenable to the development of high-throughput, semiautomated protocols.

Materials and methods

Detection of TSC2 variants in TSC patients

Mutation analysis was performed as described previously[10] or by direct sequence analysis of all *TSC1* and *TSC2* coding exons and exon/intron boundaries. In addition, both genes were analysed using the multiplex ligation-dependent probe amplification assay (MRC Holland, Amsterdam, The Netherlands). Where possible, parental DNA was collected and tested for the presence of the identified variants and, in cases of *de novo* changes, paternity testing was performed. To investigate whether the identified sequence changes had an effect on splicing, three splice site prediction programs were used.[15–17]

Materials

Expression constructs encoding the 20 TSC2 variants (G62E, R98W, 275delN, Q373P, 580delASHATRVYEMLVSHIQLHYKHSYTLP (hereafter referred to as 580del26), A607E, T1068I, T1075I, T1075T, V1199G, P1292A, S1410L, G1416D, D1512A, G1544V, 1553delTGLGRLIELKDCQPDKVYL (hereafter referred to as 1553del19), H1617Y, V1623G, R1720Q and R1720W) were derived using the Stratagene QuikChange site-directed mutagenesis kit (Stratagene, La Jolla, CA, USA). Sequence changes were numbered according to the *TSC2* cDNA as originally published, as these corresponded to the cDNA used for the expression studies.[3] Nomenclature according to the *TSC2* mutation database[18] is given in Table 1.

All variants were verified by sequencing the complete *TSC2* cDNA open reading frame. All the other constructs used in this study have been described previously.[7,19,20] Polyclonal rabbit antisera specific for human TSC1 and TSC2 have been described previously.[19] Other antibodies were purchased from Cell Signaling Technology (Danvers, MA, USA) (1A5, anti-T389 phospho-S6K mouse monoclonal; 9B11, anti-myc tag mouse monoclonal; anti-myc tag

Table 1 Summary of the ICW-based functional characterisation of 20 TSC2 variants

Nucleotide change[a]	*Amino acid change*[a]	t-*test vs wild-type*[c]	t-*test vs control*[c]	*Pathogenicity*
203G>A (185G>A)	G62E	0.555398	**0.000106**	Unclassified
310C>T (292C>T)	R98W	**0.021536**	**0.013338**	Unclassified
842delACA (824delACA)	275delN	**0.001127**	0.475101	Pathogenic
1136A>C (1118A>C)	Q373P	0.278444	**0.000072**	Pathogenic[b]
1754del78 (1736del78)	580del26	**0.002041**	0.298704	Pathogenic
1838C>A (1820C>A)	A607E	**0.003675**	0.146591	Pathogenic
3221C>T (3203C>A)	T1068I	**0.000743**	0.622030	Pathogenic
3242C>T (3224C>T)	T1075I	0.658401	**0.000909**	Unclassified
3243C>T (3225C>T)	T1075T	0.184777	**0.000057**	Unclassified
3614T>G (3596T>G)	V1199G	**0.023734**	0.175070	Pathogenic
3892C>G (3943C>G)	P1292A (P1315A)	0.290908	**0.000063**	Unclassified
4247C>T (4298C>T)	S1410L (S1433L)	0.321151	**0.000192**	Unclassified
4265G>A (4316G>A)	G1416D (G1439D)	0.332362	**0.000246**	Unclassified
4553A>C (4604A>C)	D1512A (D1535A)	**0.000139**	0.811770	Pathogenic
4649G>T (4700G>T)	G1544V (G1567V)	**0.000316**	0.424123	Pathogenic
4675del57 (4726del57)	1553del19 (1576del19)	**0.032488**	0.641493	Pathogenic
4867C>T (4918C>T)	H1617Y (H1640Y)	**0.020428**	0.148090	Pathogenic
4886T>G (4937T>G)	V1623G (V1646G)	**0.039219**	0.347325	Pathogenic
5177G>A (5228G>A)	R1720Q (R1743Q)	**0.003169**	0.960154	Pathogenic
5176C>T (5227C>T)	R1720W (R1743W)	**0.017443**	0.521431	Pathogenic

[a]Nucleotide and amino acid numbering corresponding to reference.[3] Nucleotide and amino acid numbering corresponding to reference[18] are given in parentheses.
[b]Pathogenic *de novo* mutation, most likely causing aberrant splicing of the *TSC2* mRNA; the Q373P amino acid substitution did not affect TSC1–TSC2 complex function.
[c]*P*-values <0.05 are indicated in bold.

rabbit polyclonal), Zymed laboratories (San Francisco, CA, USA) (anti-TSC1 and anti-TSC2 mouse monoclonals) and Li-Cor Biosciences (Lincoln, NE, USA) (goat anti-rabbit 680 nm and goat anti-mouse 800 nm conjugates). Chemicals were from Merck (Darmstadt, Germany), unless specified otherwise.

Cell culture

Human embryonal kidney (HEK) 293T cells were grown in Dulbecco's modified Eagle's medium (DMEM) (Lonza, Verviers, Belgium) supplemented with 10% fetal bovine serum, 50 U/ml penicillin and 50 μg/ml streptomycin (DMEM+), in a 10% CO_2 humidified incubator.

Western blotting

Cells were seeded onto 24-well plates and transfected with 0.2 μg TSC2, 0.4 μg TSC1 and 0.1 μg S6Kmyc expression constructs using polyethyleneimine (PEI) (Polysciences Inc., Warrington, PA, USA). A 1:4 w/w mixture of plasmid DNA and PEI was incubated in 0.2 ml DMEM for 15 min at 20°C before adding to the cells. After 4 h, the DMEM/DNA/PEI was replaced with DMEM+. Twenty-four hours after transfection, the cells were transferred to ice, washed with phosphate-buffered saline (PBS) (4°C) and harvested in 50 μl lysis buffer (50 mM Tris-HCl pH 8.0, 150 mM NaCl, 50 mM NaF, 1% Triton X-100, protease inhibitor cocktail (Complete, Roche Molecular Biochemicals, Woerden, The Netherlands)). Cells were lysed for 10 min on ice before centrifugation (10 000 *g* for 10 min at 4°C). The supernatants were diluted in loading buffer, separated on 6% SDS-PAGE gels and transfered to nitrocellulose membranes, as described previously.[19] Membranes were blocked for 1 h at 20°C with 5% low-fat milk powder (Campina Melkunie, Eindhoven, The Netherlands) in PBS and incubated overnight at 4°C with the primary antibodies: 1/16 000 dilution of 1895 (rabbit polyclonal against TSC2[19]), 1/5000 dilution of 2197 (rabbit polyclonal against TSC1[19]), 1/5000 dilution of a rabbit polyclonal against the myc epitope tag and 1/2000 dilution of 1A5 (mouse monoclonal against p70 S6 kinase (S6K) phosphorylated at amino acid T389). Antibodies were diluted in blocking solution containing 0.1% Tween 20 (Sigma-Aldrich Fine Chemicals, Poole, UK). After washing 3× for 5 min in PBS containing 0.1% Tween 20 (PBST), the membranes were incubated for 1 h at 20°C in the dark in PBST containing 1/5000 dilutions of goat anti-rabbit 680 nm and goat anti-mouse 800 nm secondary antibodies. After washing (3× for 5 min in PBST, 1× in PBS) the membranes were scanned using the Odyssey™ Infrared Imager (169 μm resolution, medium quality with 0 mm focus offset) (Li-Cor Biosciences, Lincoln, NE, USA). The integrated intensities of the protein bands were determined using the Odyssey™ software (default settings with background correction; 3 pixel width border average method).

ICW assays

Cells were seeded onto 96-well plates coated with 0.1 mg/ml poly-L-lysine (Sigma-Aldrich Fine Chemicals). Cells at 85–95% confluency were transfected with 0.1 μg TSC2, 0.2 μg TSC1 and 0.05 μg S6Kmyc expression constructs using PEI, as before. Each transfection mix was divided equally between three wells. After 4 h, the DMEM/DNA/PEI mixtures were replaced with DMEM+. ICW assays were performed 24 h after transfection. Cells were rinsed with PBS, fixed with freshly prepared 4% paraformaldehyde for 20 min at 20°C, washed 3× for 5 min with PBS containing 0.1% Triton X-100 and incubated for 90 min in blocking solution before incubation overnight at 4°C with the primary antibodies. Three different primary antibody mixes were prepared: 1/200 dilution of mouse monoclonal anti-TSC2 antibody, 1/200 dilution of mouse monoclonal anti-TSC1 antibody and 1/200 dilution of 1A5 (S6K T389 phosphorylation-specific mouse monoclonal). The antibodies were diluted in blocking solution containing 0.1% Tween 20 and a 1/500 dilution of the rabbit polyclonal anti-myc antibody. Antibodies were diluted according to the manufacturer's recommendations and based on the results of calibration experiments (see Supplementary Figure 1).

After washing for 3× for 5 min in PBST, the cells were incubated for 1 h at 20°C in the dark with a 1/500 dilution of goat anti-rabbit 680 nm and 1/500 dilution of goat anti-mouse 800 nm in PBST. After washing (4× for 5 min in PBST) the plates were scanned using the Odyssey Infrared Imager (169 μm resolution, medium quality with 3 mm focus offset). The integrated intensities of the protein signals were determined using the Odyssey software (8.5 mm quantification grid with background correction; 3 pixel width border average method).

ICW assay automation

In-cell western assays were performed using a Tecan EVO200 liquid handling station (Tecan Benelux, Giessen, The Netherlands). Transfected cells were fixed as before, washed 3× for 5 min with PBS containing 0.1% Triton X-100 and placed in the station for the subsequent incubation and wash steps. After aspiration of the wash buffer, the cells were incubated with blocking solution for 90 min followed by the primary antibody mixes for 8.5 h. After washing (3× for 5 min with PBST), the cells were incubated for 5 h with the secondary antibodies and washed (3× for 5 min with PBST; 1× for 5 min with PBS). Finally the PBS was aspirated, and the plate removed for scanning on the Odyssey Infrared Imager, as before. All incubation steps were performed at 4°C in the dark.

Results

ICW assay for the analysis of TSC1-TSC2-mTOR signalling

To determine whether the ICW assay was suitable for the analysis of transfected HEK 293T cells, we compared S6K

T389 phosphorylation in cells expressing TSC1, S6K and either wild-type TSC2 or the TSC2 R611Q mutant. Control cells were transfected with the pcDNA3 expression vector alone (no *TSC2*, *TSC1* or *S6K* cDNA inserts) or were co-transfected with the TSC1 and S6K expression constructs only. A schematic of the 96-well plate is shown in Figure 1a, and the resulting scans are shown in Figure 1b. After subtraction of the background signals, the ratio of the TSC2, TSC1 or T389-phosphorylated S6K (T389) signal (green) to the total S6K signal (red) was determined (Figure 1c). S6K-T389 phosphorylation was reduced ~2-fold in cells expressing wild-type TSC2, compared to either cells expressing the R611Q mutant or to cells without TSC2 expression. A similar reduction in S6K-T389 phosphorylation was observed when the protocol was modified for the Tecan EVO200 liquid handling station (Figure 1d).

ICW analysis of TSC2 variants

Next, we tested 20 TSC2 variants identified in our patient cohort, including three in-frame deletions (275delN, 580del26 and 1553del19), 17 missense changes (G62E, R98W, Q373P, A607E, T1068I, T1075I, V1199G, P1292A, S1410L, G1416D, D1512A, G1544V, H1617Y, V1623G, R1720Q and R1720W) and one silent change (T1075T). Two of the variants, R1720Q and R1720W, had previously been shown to be *de novo* changes occurring in sporadic TSC patients and, on this basis, were assumed to be pathogenic mutations.[10,18] In the other 18 cases, essential genetic and/or clinical data were unavailable and the identified variants could not be classified as either pathogenic or non-pathogenic. The positions of the variant amino acids are indicated in Figure 2.

All variants were analysed using the ICW assay in three independent experiments. The integrated intensities of the fluorescent signals were quantified using the Odyssey software and the signals for each TSC2 variant, and for TSC1 and T389-phosphorylated S6K in the presence of the different variants were determined relative to the total S6K signal in the same well. Subsequently, the degree of S6K-T389 phosphorylation in the presence of the different TSC2 variants, relative to wild-type TSC2, was determined.

A representative scan is shown in Figure 3b. The total S6K signal was relatively constant across the different wells, indicating that inter-well differences in transfection efficiency and cell number were small. The signals for the different TSC2 variants were also relatively constant. None of the amino acid changes had a dramatic effect on the TSC2 signal, although a slight decrease was noted for the R611Q, 275delN, 580del26, A607E and V1623G variants. Similarly, the TSC1 signal was relatively constant, with only slight reductions in the presence of the TSC2 R611Q, 275delN, 580del26 and A607E variants. The T389 phosphorylation status of S6K was clearly dependent on the presence of the different TSC2 variants. TSC2-dependent inhibition of S6K-T389 phosphorylation was significantly reduced (ie, specific S6K T389 phosphorylation signal was increased compared to wild-type TSC2) in the presence of the R98W, 275delN, 580del26, A607E, T1068I, V1199G, D1512A, G1544V, 1553del19, H1617Y, V1623G, R1720Q and R1720W variants. As shown in Table 1, the T389/S6K ratio in the presence of these TSC2 variants was significantly different to the T389/S6K ratio in the presence of wild-type TSC2 (unpaired *t*-test $P<0.05$). Furthermore, in the presence of these variants, S6K T389 phosphorylation was comparable to T389 phosphorylation in the absence of TSC2 or in the presence of the TSC2 R611Q mutant (T389/S6K ratio was not significantly different from control: unpaired *t*-test $P>0.05$; Table 1). Only the R98W variant was significantly different from both the positive and negative controls (Figure 3 and Table 1). The G62E, Q373P, T1075I, T1075T, P1292A, S1410L and G1416D variants were as effective as wild-type TSC2 at inhibiting S6K T389 phosphorylation (T389/S6K ratio was not significantly different from wild-type TSC2: unpaired *t*-test $P>0.05$; T389/S6K ratio was significantly different from the T389/S6K ratio in the absence of TSC2: unpaired *t*-test $P<0.05$; Table 1).

Immunoblot analysis of the TSC2 variants

We analysed the effects of the TSC2 variants on mTOR activity by immunoblotting. In three independent experiments, the expression of TSC1 and the TSC2 variants, and the expression and T389 phosphorylation status of S6K

Figure 1 Optimisation of the ICW assay for analysis of TSC2 variants. (**a**) Schematic showing part of a 96-well cell culture plate. Cells in wells A1–A3 (row A) were transfected with expression constructs for wild-type TSC2, TSC1 and myc-tagged S6K (S6K); B1–B3 (row B) were transfected with expression constructs for the TSC2 R611Q variant, TSC1 and S6Kmyc; C1–C3 (row C) with vector only and D1–D3 (row D) with expression constructs for TSC1 and S6Kmyc only. A1–D1 (column 1) were probed with a monoclonal antibody specific for TSC2 (Zymed laboratories; green); A2–D2 (column 2) were probed with a monoclonal antibody specific for TSC1 (Zymed laboratories; green) and A3–D3 (column 3) were probed with a monoclonal antibody specific for T389-phosphorylated S6K (Cell Signaling Technology; green). All wells were probed with a polyclonal antibody specific for the S6K myc tag (Cell Signaling Technology; red). (**b**) Odyssey scans of the wells are shown in A, showing the 800 nm (green) channel (left), the 680 nm (red) channel (centre) and the merged image (right). The transfections in rows A, B and C are indicated on the right, the antibody signals revealed in columns 1, 2 and 3 are indicated below the scans. (**c**) Graphical representation of the scans is shown in B. The integrated intensities of the green and red fluorescent signals were determined using the Odyssey software. After subtraction of the background values (wells C1–C3; row C), the green:red ratio was calculated. (**d**) ICW assay using the Tecan EVO200 liquid handling station. Integrated intensities were determined and the green:red signal ratios calculated as in C for four separate transfection experiments. The mean TSC2/S6K, TSC1/S6K and T389/S6K ratios, and standard deviations are indicated. The mean T389/S6K ratio in the presence of wild-type TSC2 was significantly reduced compared to the TSC2 R611Q variant ($P=0.03$) and TSC1 only control ($P=0.004$).

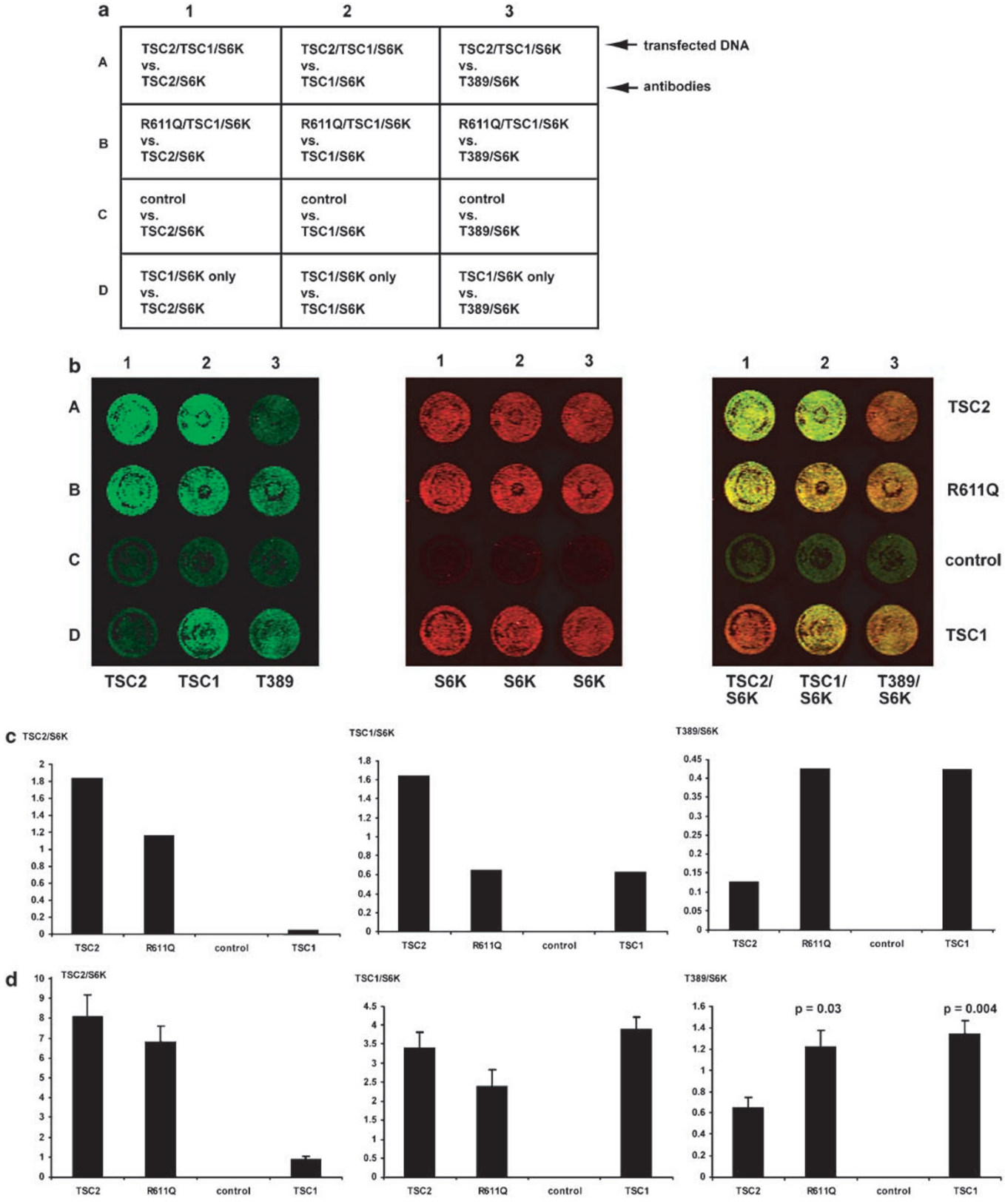
a
1
2
3
A
B
C
D
TSC2/TSC1/S6K vs. TSC2/S6K
TSC2/TSC1/S6K vs. TSC1/S6K
TSC2/TSC1/S6K vs. T389/S6K
R611Q/TSC1/S6K vs. TSC2/S6K
R611Q/TSC1/S6K vs. TSC1/S6K
R611Q/TSC1/S6K vs. T389/S6K
control vs. TSC2/S6K
control vs. TSC1/S6K
control vs. T389/S6K
TSC1/S6K only vs. TSC2/S6K
TSC1/S6K only vs. TSC1/S6K
TSC1/S6K only vs. T389/S6K
transfected DNA
antibodies
b
TSC2
TSC1
T389
S6K
S6K
S6K
TSC2/ S6K
TSC1/ S6K
T389/ S6K
TSC2
R611Q
control
TSC1
c
TSC2/S6K
TSC1/S6K
T389/S6K
TSC2
R611Q
control
TSC1
d
TSC2/S6K
TSC1/S6K
T389/S6K
p = 0.03
p = 0.004

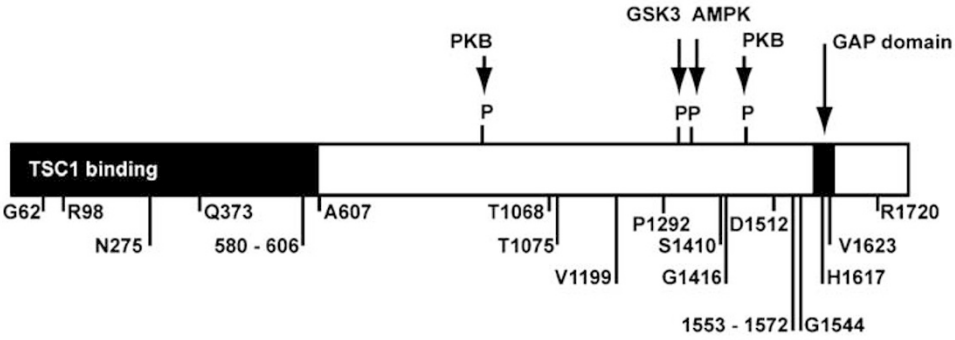

Figure 2 Schematic diagram of TSC2, showing the TSC1-binding and GAP domains, prominent sites of PKB, GSK3 and AMPK phosphorylation, and the positions of the variant amino acids tested in this study.

were determined (Figure 4). The results of the immunoblotting experiments were consistent with the ICW assays. Compared to wild-type TSC2 and the G62E, Q373P, T1075I, T1075T, P1292A, S1410L and G1416D variants, S6K T389 phosphorylation was increased in the presence of the R98W, 275delN, 580del26, A607E, T1068I, V1199G, D1512A, G1544V, 1553del19, H1617Y, V1623G, R1720Q and R1720W variants. The immunoblot data differed from the ICW data in that larger differences were detected in the signals of the different TSC2 variants, and in the TSC1 signal in the presence of the different TSC2 variants. The S6K signal was relatively constant, indicating that the observed differences were unlikely to be due to differences in cell number and transfection efficiency between the variants. Compared to wild-type TSC2, the signal for the R611Q variant was consistently reduced. In addition, the TSC1 signal was also reduced in the presence of the R611Q variant. Previous studies have demonstrated that the R611Q mutation disrupts the TSC1–TSC2 interaction, reducing the levels of TSC1 and TSC2 in cytosolic fractions.[20] A similar pattern was observed for the R98W, 275delN, 580del26 and A607E variants, indicating that these variants also have a reduced ability to interact with TSC1. The amino acids affected in these variants all map to regions of TSC2 that have previously been shown to be important for the TSC1–TSC2 interaction.[20–22]

Wild-type TSC2 was detected as a broad band on the immunoblots, consisting of 2–3 isoforms with slightly different migration characteristics. In contrast, some of the TSC2 variants appeared to migrate as a single band. This is most likely due to differences in the post-translational modification of the different variants.[7] We compared the phosphorylation status of the different variants using an antibody specific for TSC2 phosphorylated at the T1439 position. However, using this antibody, we did not observe any clear differences in TSC2-T1439 phosphorylation between wild-type TSC2 and the TSC2 variants (see Supplementary Figure 2).

Although the immunoblotting experiments supported the ICW data, the differences averaged over three independent experiments were not always significant (unpaired *t*-test; Figure 4). Therefore, the ICW gave more consistent and reproducible data, and allowed us to classify the 20 variants as pathogenic or not in a relatively short period of time. The ICW required fewer manipulations than the immunoblot analysis and was always performed using the same 96-well grid. Variables such as the cell harvest and fractionation steps and the gel and buffer characteristics most likely resulted in more inter-experiment differences in the immunoblot assays. A comparison of the steps involved in the two techniques is shown in Figure 5.

The ICW assay indicated that the TSC2 275delN, 580del26, A607E, T1068I, V1199G, D1512A, G1544V, 1553del19, H1617Y, V1623G, R1720Q and R1720W variants were likely to be pathogenic, as they all disrupted the ability of the TSC1–TSC2 complex to inhibit mTOR activity. Immunoblot analysis confirmed that these 12 variants are inactive and therefore disease causing.

The G62E, Q373P, T1075I, T1075T, P1292A, S1410L and G1416D variants were indistinguishable from wild-type TSC2 in both the ICW and immunoblot assays. However, it was possible that the corresponding nucleotide changes could still be pathogenic through effects on *TSC2* mRNA splicing. We analysed the nucleotide changes using three splice site prediction programs.[15–17] Only the 1136A>C (Q373P, *TSC2* exon 10) substitution was predicted to affect splicing. Codon 373 is encoded by the last three nucleotides of *TSC2* exon 10, and according to all three prediction programs, the 1136A>C substitution disrupts the exon 10 donor sequence, resulting in an aberrantly spliced *TSC2* mRNA. We concluded that the 1136A>C (Q373P) variant was a pathogenic splice site mutation, and not a missense mutation. Subsequent genetic analysis of the parents of the TSC patient with the *TSC2* 1136A>C (Q373P) variant demonstrated that this was a *de novo* change. Paternity was also confirmed in this case (data not shown).

In contrast to the TSC2 variants discussed above, the R98W variant could not be classified as either pathogenic or non-pathogenic. This variant was able to inhibit S6K T389 phosphorylation in both the ICW and immunoblot

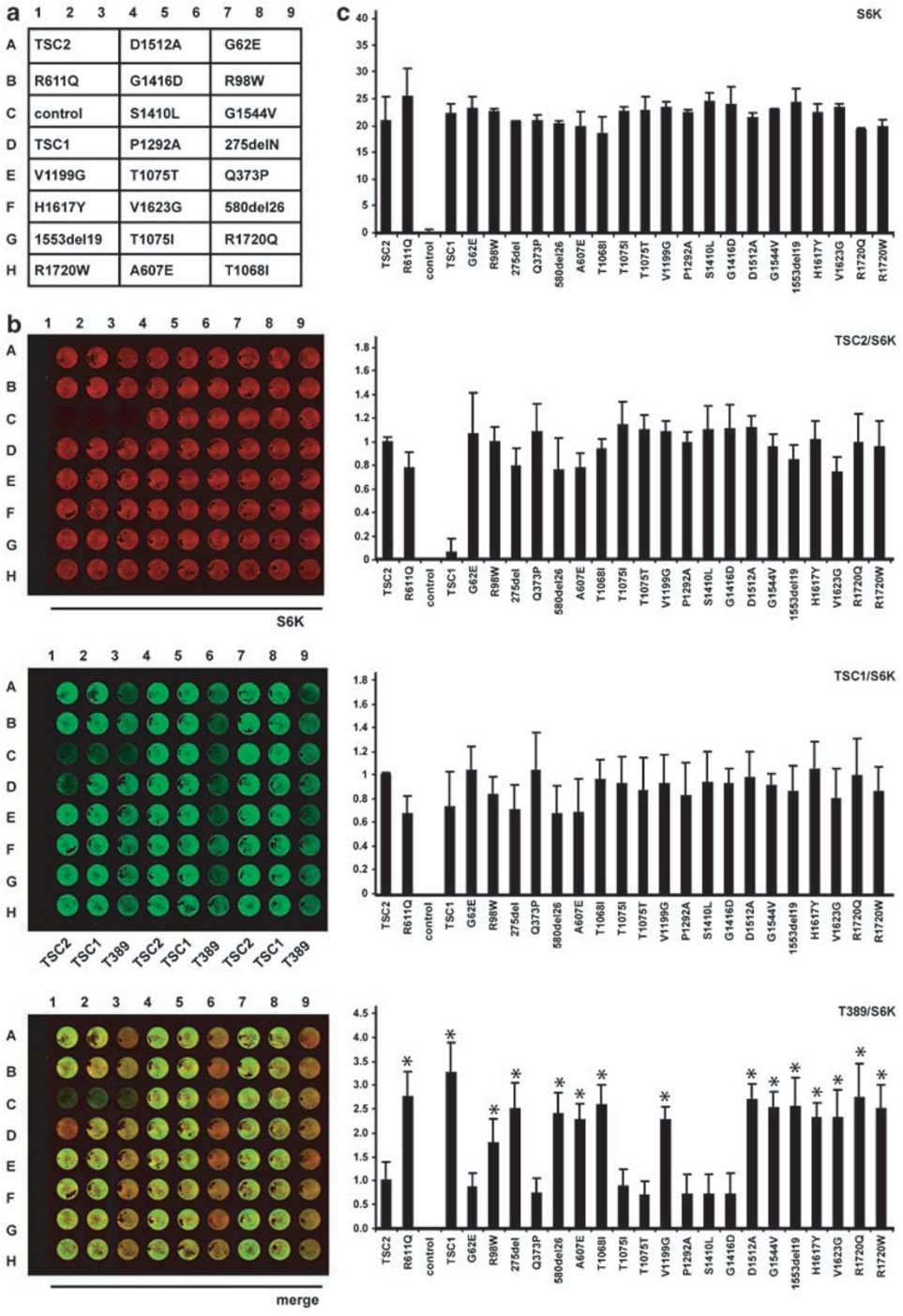

Figure 3 Characterisation of 20 TSC2 variants using the ICW assay. (**a**) Schematic showing part of a 96-well cell culture plate. Cells in wells A1–A3 (row A), B1–B3 (row B), C1–C3 (row C) and D1–D3 (row D) were transfected as before (see Figure 1). Cell in the remaining sets of three wells were transfected with expression constructs for the different TSC2 variants, TSC1 and S6Kmyc. All wells were probed with a polyclonal antibody specific for the S6K myc tag (red). Wells in columns 1, 4 and 7 were probed with a monoclonal antibody specific for TSC2 (green); wells in columns 2, 5 and 8 were probed with a monoclonal antibody specific for TSC1 (green) and wells in columns 3, 6 and 9 were probed with a monoclonal antibody specific for T389-phosphorylated S6K (green). (**b**) Odyssey scans of the wells are shown in (**a**). (**c**) Graphical representation of the results of three independent ICW assays. The integrated intensities of the green and red fluorescent signals were determined using the Odyssey software. In each case the background values, measured in wells C1–C3 (control), were subtracted from the integrated intensity. In the top graphic, the mean integrated intensity values for S6K are shown. In the three lower graphics, the expression of TSC2 and TSC1, and the T389 phosphorylation of S6K are indicated. To correct for inter-well differences in cell number and transfection efficiency, values are expressed relative to the total S6K signal. Standard deviations are indicated. TSC2 variants with a significantly different T389/S6K ratio than wild type ($P<0.05$) are indicated with an asterisk.

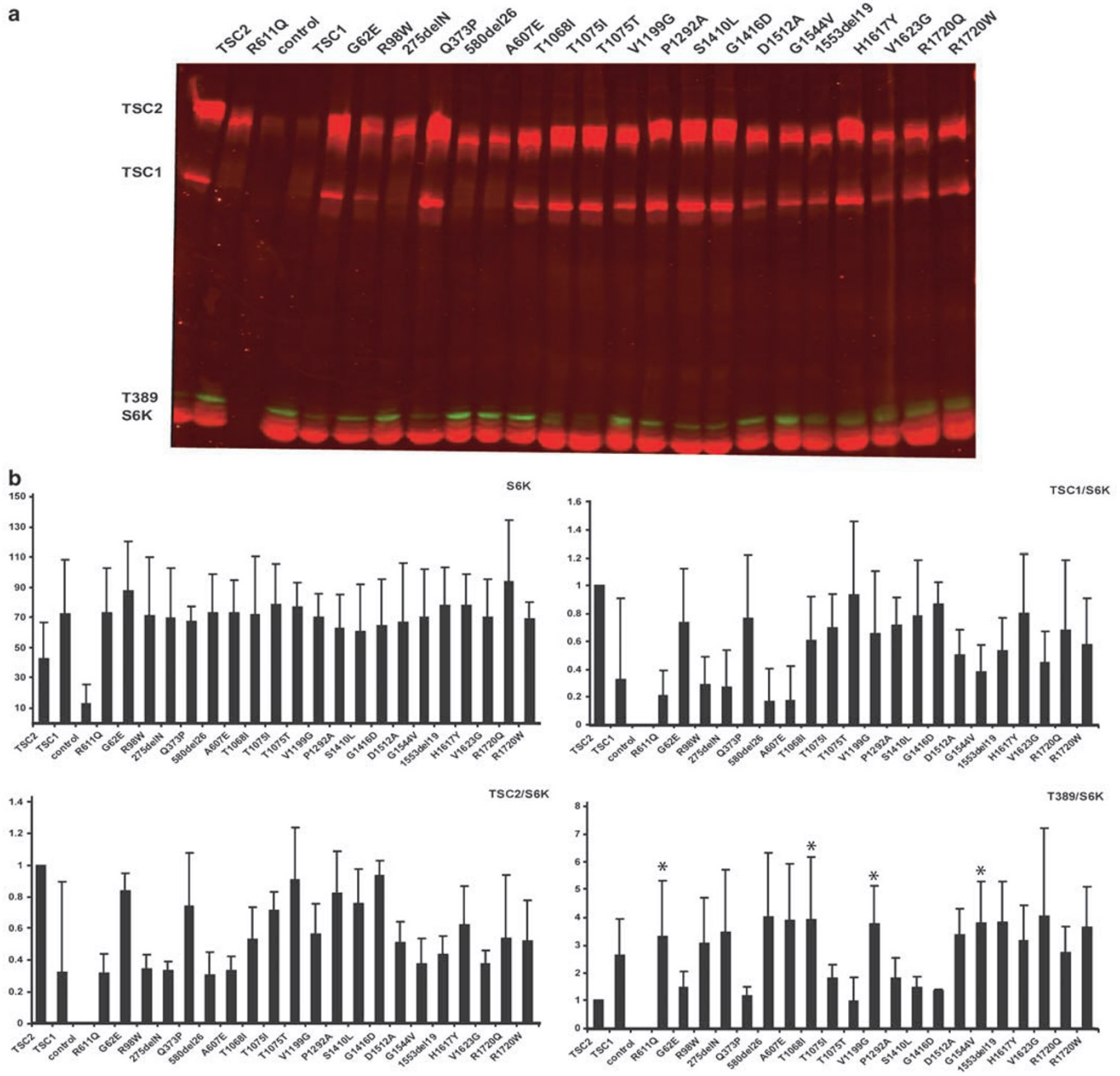

Figure 4 Characterisation of 20 TSC2 variants by immunoblot analysis. Cells co-transfected with expression constructs encoding TSC1, S6Kmyc and either wild-type TSC2 or one of the 20 TSC2 variants were harvested and cytosolic fractions separated on a 6% SDS-PAGE gel before transfer. Blots were probed with rabbit polyclonal antisera against TSC2, TSC1 and the myc epitope tag, and a mouse monoclonal against T389-phosphorylated S6K, followed by the Li-Cor goat anti-rabbit 800 and goat anti-mouse 680 secondary antibodies. (**a**) Representative scan of an immunoblot. Expression of the TSC2 variants, TSC1 and S6K (all red) and the T389 phosphorylation of S6K (green) are indicated. (**b**) Graphical representation of the results of three independent immunoblots. The integrated intensities of the green and red fluorescent signals were determined using the Odyssey software with background correction. In the top graphic, the mean values for S6K are shown. In the three lower graphics, the expression of TSC2 and TSC1, and the T389 phosphorylation of S6K are indicated. To correct for differences in cell number and transfection efficiency, values are expressed relative to the total S6K signal per lane. Standard deviations are indicated. TSC2 variants with a significantly different T389/S6K ratio than wild type ($P<0.05$) are indicated with an asterisk.

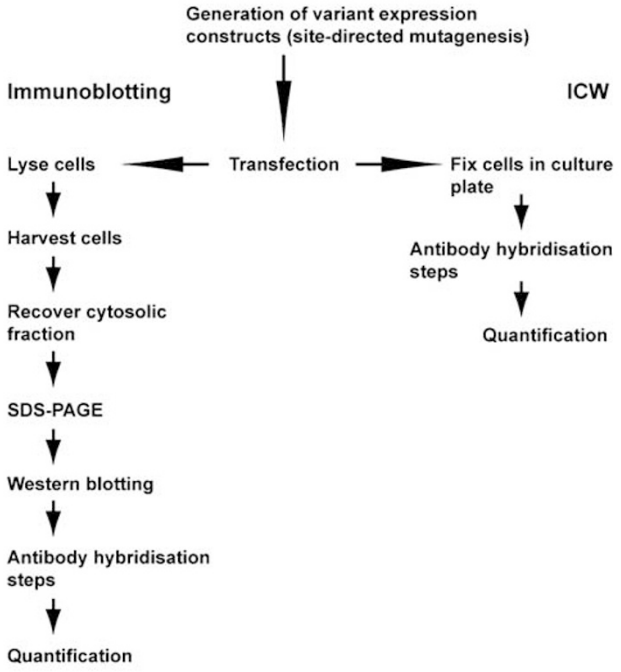

Figure 5 Flow diagram to show the steps involved in the ICW assay, compared to immunoblotting.

assays, but was less effective than wild-type TSC2. On the immunoblots, the expression of the R98W variant was reduced compared to wild-type TSC2, and the expression of TSC1 was also consistently reduced in the presence of this variant. This suggests that the R98W substitution affects the TSC1–TSC2 interaction, and therefore reduces the ability of the complex to inhibit mTOR signalling.

As shown in Figure 6, the *TSC2* 310C>T (R98W) substitution was detected in a mother and a fetus. The fetus did not survive to term and was diagnosed with TSC post-mortem. No signs of TSC were reported in either parent. The mother was heterozygous for the *TSC2* 310C>T (R98W) variant, whereas the fetus appeared to be hemizygous for this variant as the wild-type allele was not detected and MLPA analysis of the fetal DNA indicated that there was a deletion of *TSC2* exons 1–8. MLPA analysis of the *TSC1* locus in the fetus suggested that there was also a duplication of the entire *TSC1* coding region. However, due to a lack of material, we were unable to confirm the MLPA data. Therefore, the clinical, genetic and functional data for this variant were all problematic and we were unable to determine for certain whether the R98W substitution disrupts the TSC1–TSC2 complex sufficiently to cause TSC. *TSC2* missense mutations with apparently mild phenotypic effects have been described previously,[23–25] and have been shown to affect TSC1–TSC2 function *in vitro*.[24,25] In the family shown in Figure 6, it seems most likely that the deletion of exons 1–8 at the *TSC2* locus

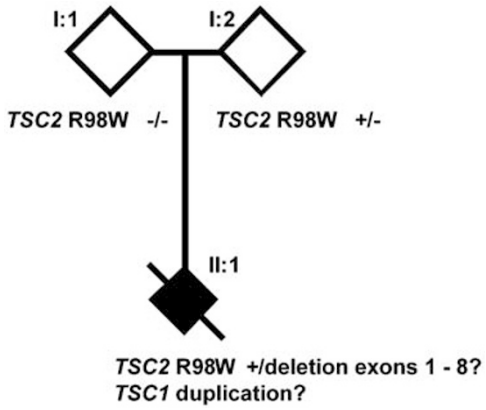

Figure 6 Pedigree showing inheritance of the TSC2 310 C>T (R98W) variant. Open symbols indicate no signs or symptoms of TSC; black symbol indicates definite TSC (diagnosed post-mortem). Genotypes, where known, are indicated.

caused TSC in the fetus. We could not rule out the possibility that the TSC2 R98W substitution modifies the phenotype in this family.

Discussion

Mutation analysis of individuals with, or suspected of having, a genetic disease facilitates the diagnosis, treatment and genetic counselling of those individuals and their families. However, in some cases, it is not possible to determine from the genetic data whether an identified nucleotide change is disease causing. Functional analysis of the predicted protein variants provides an additional method for determining whether specific changes are pathogenic. Here, we show that the ICW assay is a robust and reproducible assay for the analysis of unclassified TSC2 variants and can complement standard DNA-based molecular diagnostics. We tested the activity of 20 different TSC2 variants and identified 12 pathogenic changes (275delN, 580del26, A607E, T1068I, V1199G, D1512A, G1544V, 1553del19, H1617Y, V1623G, R1720Q and R1720W), 7 neutral variants (G62E, Q373P, T1075I, T1075T, P1292A, S1410L and G1416D), and one variant (R98W) where the functional significance of the substitution was not clear.

Characterisation of the effects of different TSC2 amino acid changes on the TSC1–TSC2 complex will help provide insight into the structure and function of the complex. The N-terminal 769 amino acids of TSC2 are important for the TSC1–TSC2 interaction.[19,22] Four changes mapping to this domain (R98W, 275delN, 580del26 and A607E) reduced the levels of both TSC1 and TSC2 in cytosolic fractions. We did not observe any effect of either the G62E or Q373P substitutions, indicating that these residues are not critical for the TSC1–TSC2 interaction. We analysed seven TSC2

variants affecting amino acids close to the TSC2 GAP domain (amino acids 1593–1631)[3] (Figure 2). All of these changes prevented the TSC1–TSC2-dependent inhibition of mTOR signaling, indicating that residues within and flanking the reported GAP domain are essential for TSC2 activity.

The TSC is one of several diseases that are caused by mutations in genes involved in the mTOR signalling pathway.[26] The application of similar ICW assays to analyse unclassified variants in individuals with these diseases may also prove to be a useful adjunct to standard molecular genetic analysis.

Acknowledgements

Financial support was provided by the US Department of Defense Congressionally-Directed Medical Research Program (grant no. TS060052), and the Michelle Foundation. The authors report no conflicts of interest.

References

1 Gomez M, Sampson J, Whittemore V (eds): *The Tuberous Sclerosis Complex*. Oxford, UK: Oxford University Press, 1999, pp 10–23.
2 van Slegtenhorst M, de Hoogt R, Hermans C *et al*: Identification of the tuberous sclerosis gene *TSC1* on chromosome 9q34. *Science* 1997; **277**: 805–808.
3 The European Chromosome 16 Tuberous Sclerosis Consortium: Identification and characterization of the tuberous sclerosis gene on chromosome 16. *Cell* 1993; **75**: 1305–1315.
4 Li Y, Corradetti MN, Inoki K, Guan K-L: TSC2: filling the GAP in the mTOR signaling pathway. *Trends Biochem Sci* 2004; **29**: 32–38.
5 Zhang H, Cicchetti G, Onda H *et al*: Loss of Tsc1/Tsc2 activates mTOR and disrupts PI3K-Akt signaling through downregulation of PDGFR. *J Clin Invest* 2003; **112**: 1223–1233.
6 Kwiatkowski DJ, Zhang H, Bandura JL *et al*: A mouse model of TSC1 reveals sex-dependent lethality from liver hemangiomas, and up-regulation of p70S6 kinase activity in *Tsc1* null cells. *Hum Mol Genet* 2001; **11**: 525–534.
7 Nellist M, Sancak O, Goedbloed MA *et al*: Distinct effects of single amino acid changes to tuberin on the function of the tuberin-hamartin complex. *Eur J Hum Genet* 2005; **13**: 59–68.
8 Jones AC, Shyamsundar MM, Thomas MW *et al*: Comprehensive mutation analysis of *TSC1* and *TSC2*, and phenotypic correlations in 150 families with tuberous sclerosis. *Am J Hum Genet* 1999; **64**: 1305–1315.
9 Dabora SL, Jozwiak S, Franz DN *et al*: Mutational analysis in a cohort of 224 tuberous sclerosis patients indicates increased severity of *TSC2*, compared with *TSC1*, disease in multiple organs. *Am J Hum Genet* 2001; **68**: 64–80.
10 Sancak O, Nellist M, Goedbloed M *et al*: Mutational analysis of the *TSC1* and *TSC2* genes in a diagnostic setting: genotype-phenotype correlations and comparison of diagnostic DNA techniques in tuberous sclerosis complex. *Eur J Hum Genet* 2005; **13**: 731–741.
11 Au K-S, Williams AT, Roach ES *et al*: Genotype/phenotype correlation in 325 individuals referred for a diagnosis of tuberous sclerosis complex in the United States. *Genet Med* 2007; **9**: 88–100.
12 Nellist M, Sancak O, Goedbloed M *et al*: Functional characterisation of the TSC1-TSC2 complex to assess multiple *TSC2* variants identified in single families affected by tuberous sclerosis complex. *BMC Med Genet* 2008; **9**: 10.
13 Wong SK: A 384-well cell-based phospho-ERK assay for dopamine D2 and D3 receptors. *Anal Biochem* 2004; **333**: 265–272.
14 Selkirk JV, Nottebaum LM, Ford IC *et al*: A novel cell-based assay for G-protein-coupled receptor-mediated cyclic adenosine monophosphate response element binding protein phosphorylation. *J Biomol Screen* 2006; **11**: 351–358.
15 NetGene2 Server. [www.cbs.dtu.dk/services/NetGene2].
16 SpliceSiteFinder. [www.genet.sickkids.on.ca/~ali/splicesitefinder.html].
17 BDGP. Splice Site Prediction by Neural Network [www.fruitfly.org/seq_tools/splice.html].
18 Tuberous sclerosis database—Leiden Open Variation Database. [www.chromium.liacs.nl/lovd/index.php?select_db=TSC2].
19 van Slegtenhorst M, Nellist M, Nagelkerken B *et al*: Interaction between hamartin and tuberin, the *TSC1* and *TSC2* gene products. *Hum Mol Genet* 1998; **7**: 1053–1057.
20 Nellist M, Verhaaf B, Goedbloed MA, Reuser AJJ, van den Ouweland AMW, Halley DJJ: *TSC2* missense mutations inhibit tuberin phosphorylation and prevent formation of the tuberin-hamartin complex. *Hum Mol Genet* 2001; **10**: 2889–2898.
21 Hodges A, Li S, Maynard J *et al*: Pathological mutations in TSC1 and TSC2 disrupt the interaction between hamartin and tuberin. *Hum Mol Genet* 2001; **10**: 2899–2905.
22 Li Y, Inoki K, Guan K-L: Biochemical and functional characterizations of small GTPase rheb and TSC2 GAP activity. *Mol Cell Biol* 2004; **24**: 7965–7975.
23 O'Conner SE, Kwiatkowski DJ, Roberts PS, Wollmann RL, Huttenlocher PR: A family with seizures and minor features of tuberous sclerosis and a novel TSC2 mutation. *Neurology* 2003; **61**: 409–412.
24 Mayer K, Goedbloed M, van Zijl K, Nellist M, Rott HD: Characterisation of a novel TSC2 missense mutation in the GAP related domain associated with minimal clinical manifestations of tuberous sclerosis. *J Med Genet* 2004; **41**: e64.
25 Jansen A, Sancak O, D'Agostino D *et al*: Mild form of tuberous sclerosis complex is associated with TSC2 R905Q mutation. *Ann Neurol* 2006; **60**: 528–539.
26 Inoki K, Corradetti MN, Guan K-L: Dysregulation of the TSC-mTOR pathway in human disease. *Nat Genet* 2005; **37**: 19–24.

Supplementary Information accompanies the paper on European Journal of Human Genetics website (http://www.nature.com/ejhg)